The Unreasonable Efficiency of Total Rain Evaporation Removal in Triggering Convective Self-Aggregation

Y.-L. Hwong[1], C.J. Muller[1]

[1]Institute of Science and Technology Austria, Klosterneuburg, Austria

Key Points:

- When rain evaporation is removed in the PBL, convective self-aggregation (CSA) is triggered by convective heating of the moist regions
- Surprisingly, CSA only occurs when rain evaporation is almost totally removed in the PBL, due to opposing temperature and moisture effects
- CSA occurs more easily in a larger domain due to stronger radiatively-induced subsidence, while cold pools play a less significant role

Corresponding author: Yi-Ling Hwong, `yiling.hwong@gmail.com`

Abstract

The elimination of rain evaporation in the planetary boundary layer (PBL) has been found to lead to convective self-aggregation (CSA) even without radiative feedback, but the precise mechanisms underlying this phenomenon remain unclear. We conducted cloud-resolving simulations with two domain sizes and progressively reduced rain evaporation in the PBL. Surprisingly, CSA only occurred when rain evaporation was almost completely removed. The additional convective heating resulting from the reduction of evaporative cooling in the moist patch was found to be the trigger, thereafter a dry subsidence intrusion into the PBL in the dry patch takes over and sets CSA in motion. Temperature and moisture anomalies oppose each other in their buoyancy effects, hence explaining the need for almost total rain evaporation removal. We also found radiative cooling and not cold pools to be the leading cause for the comparative ease of CSA to take place in the larger domain.

Plain Language Summary

Convective clouds are not randomly scattered across the sky but tend to clump together, a phenomenon known as convective self-aggregation (CSA). The interaction between clouds and radiation is a key mechanism for CSA to occur. Curiously, CSA can still take place without this radiative feedback, provided that rain is prohibited from evaporating in the lowest layers of the atmosphere ($\sim$1 km), called the planetary boundary layer (PBL). To investigate the physical processes behind this type of CSA (no-evaporation CSA, or "NE-CSA"), we ran high resolution atmospheric model simulations and reduced rain evaporation in steps in the PBL. We found that the additional heat resulting from the reduction of evaporative cooling is crucial in triggering NE-CSA, thereafter the invasion of dry air into the PBL in the dry region takes over and intensifies aggregation. Surprisingly, allowing even a minuscule amount of rain to evaporate prevents NE-CSA from taking place. This is because removing rain evaporation has two opposing effects on convection: heating and drying. The former aids convection while the latter hinders it. Only when rain evaporation is almost completely eliminated can the heating effect be powerful enough to overcome the drying effect and kick-start NE-CSA.

1 Introduction

Convective self-aggregation (CSA), an atmospheric intrigue where deep convective clouds spontaneously organize into clusters under homogeneous radiative-convective equilibrium (RCE) conditions devoid of external forcing, has been extensively studied in cloud-resolving models (CRMs) (see Muller et al., 2022; Wing et al., 2018, for comprehensive reviews). These studies investigated myriad aspects of CSA in RCE, including its time and length scales (Patrizio & Randall, 2019; Wing & Cronin, 2016; Yanase et al., 2020), onset and maintenance mechanisms (Muller & Bony, 2015 [henceforth MB15]; Wing & Emanuel, 2014), impact on mean climate (Bretherton et al., 2005; Wing & Cronin, 2016) and climate sensitivity (Cronin & Wing, 2017; Wing, 2019; Wing et al., 2020), and relevance to tropical meteorology such as the Madden-Julian Oscillation (MJO; Arnold & Randall, 2015; Khairoutdinov & Emanuel, 2018) and tropical cyclones (Carstens & Wing, 2020; Muller & Romps, 2018). In CRM simulations, CSA has been found to manifest itself more readily in larger domains and coarser resolutions (Muller & Held, 2012; Yanase et al., 2020).

Radiative feedback has been found to be a crucial ingredient for CSA (MB15; Wing & Emanuel, 2014), while surface flux feedback is a favorable but not indispensable condition (Holloway & Woolnough, 2016; Muller & Held, 2012). The role of moisture has also been studied, including its effect on the dynamics of CSA (D. Yang, 2018), the importance of dry-subsidence feedback in dry patch intensification (B. Yang & Tan, 2020), and the development of CSA through a moisture coarsening process (Craig & Mack, 2013;

Windmiller & Craig, 2019). Generally, CSA has been associated with physical processes that generate a low-level circulation leading to an upgradient transport of moist static energy (MSE) from dry to moist regions (Bretherton et al., 2005; Naumann et al., 2017; Yanase et al., 2022). However, the role of and precise mechanisms producing this circulation remain ambiguous: shallow circulation has been argued to hamper CSA from developing in smaller domains (Jeevanjee & Romps, 2013); its strength and importance have been found to be model dependent (Cerlini et al., 2023); questions also remain whether it is radiatively (Muller & Held, 2012; Naumann et al., 2017) or convectively driven (Holloway & Woolnough, 2016).

Rain evaporation has also been found to impact CSA. When rain evaporation is disabled in the PBL, CSA can occur even in the absence of radiative and surface flux feedbacks (Holloway & Woolnough, 2016; MB15; D. Yang, 2019). The physical mechanisms underlying this type of CSA—referred to here as "no-evaporation CSA" (NE-CSA)—is still unclear and is the focus of this study. Several processes have been proposed to be responsible for NE-CSA. MB15 referred to NE-CSA as "moisture-memory aggregation" and suggested that the feedback between clouds and the environmental water vapor potentially underlies this type of aggregation. Another process known to affect convective organization is entrainment (Mapes & Neale, 2011; Tompkins, 2001; Tompkins & Semie, 2017): the entrainment of moist environmental air stimulates convection, which in turn moistens the environment through detrainment, representing a positive feedback that could organize convection into clusters. However, D. Yang (2019) showed that NE-CSA can still occur without entrainment-related feedback. Instead, the author proposed that the convective heating-overturning circulation (CHOC) feedback is responsible for generating the available potential energy (APE) necessary for NE-CSA to develop.

Another hypothesis for NE-CSA relates to cold pools, which many studies have shown to have a hindering effect on CSA (e.g., Nissen & Haerter, 2021; Yanase et al., 2020). Jeevanjee and Romps (2013) showed that convection always self-aggregated regardless of domain sizes when rain evaporation was removed in the lowest 1 km. The authors hypothesized that cold pools inhibit CSA by homogenizing the PBL properties between dry and moist areas. Eliminating cold pools hence eased the occurrence of CSA. However, D. Yang (2018) used scale analyses to show that cold pools are not the reason for NE-CSA but the decrease in evaporative cooling and associated increase in APE is the more likely cause.

Given the lack of consensus in this area, the goal of our study is to investigate the mechanisms underlying NE-CSA. Instead of completely removing rain evaporation in the PBL—which represents a dramatic perturbation to the system—we progressively reduced rain evaporation and observed the impact on CSA. Our research questions are:

1. How does CSA change when rain evaporation is reduced in the PBL?
2. Which physical processes are involved in the development of CSA when rain evaporation is reduced or removed in the PBL?

2 Methods

2.1 Model and Simulation Setup

We performed 3-D simulations with the System for Atmosphere Modeling (SAM) CRM (version 6.10.8; Khairoutdinov & Randall, 2003). SAM solves the anelastic conservation equations of momentum, mass, energy and water. Non-rotating RCE simulations over an ocean surface were conducted, with a constant sea-surface temperature of 301 K. Diurnal cycle was disabled by setting the solar constant and zenith angle to values of 685 W m^{-2} and 51.7° (following Tompkins & Craig, 1998), respectively. To focus on the rain evaporation feedback, we disabled radiative and surface flux feedbacks by hor-

izontally homogenizing radiative cooling rates and surface fluxes at every time step. The SAM one-moment microphysics parameterization was used. Two domain sizes were tested: 128 × 128 km ($\Delta x = 1$ km; denoted as L128) and 256 × 256 km ($\Delta x = 4$ km; L256). A 64 level stretched vertical grid was used, with the model bottom and top at 37.5 m and 27 km, respectively. A sponge layer with Newtonian relaxation to no motion was applied in the top third of the domain to avoid unrealistic gravity wave build-up. All simulations were run for 40 days.

2.2 Rain Evaporation Reduction

Following MB15, we changed the amount of rain evaporation by multiplying the evaporation of precipitating water by a factor of α in the lowest 1 km. We first conducted a set of experiments where rain evaporation was progressively reduced in steps of $\alpha =$ [0.8, 0.6, 0.4, 0.2, 0]. Surprisingly, we found that convection became disaggregated even at $\alpha = 0.2$. Further reduction of rain evaporation showed that CSA only occurred when rain evaporation was almost completely removed, and the α values for convection to transition from a scattered to an aggregated state were smaller for L128 than L256 by around an order of magnitude. In view of this, we conducted a new set of experiments by setting $\alpha =$ [0.05, 0.02, 0.01, 0.005, 0.002, 0.001, 0] for L128 and $\alpha =$ [0.5, 0.2, 0.1, 0.05, 0.02, 0.01, 0] for L256. Additionally, we ran control experiments with $\alpha = 1$ for both homogenized and interactive radiation.

2.3 Buoyancy Analyses

A high (low) surface pressure anomaly of the dry (moist) patch and the associated buoyancy anomalies are necessary to establish a shallow circulation frequently linked to CSA (Shamekh et al., 2020; D. Yang, 2018). Assuming a weak temperature (and buoyancy) gradient (WTG) in the free troposphere (FT) (Sobel et al., 2001), our analyses focus primarily on the generation of buoyancy anomalies in the PBL and the physical processes that could amplify these anomalies. Following D. Yang (2018), we used virtual potential temperature as a proxy for buoyancy as related by

$$b = g\frac{\theta_v^{'}}{\overline{\theta}_v} \approx g\left(\frac{\theta^{'}}{\overline{\theta}} + \frac{\epsilon q_v^{'}}{1+\overline{q}_v}\right) \tag{1}$$

where b is the buoyancy, g the gravitational acceleration, $\theta_v^{'}$ and $\theta^{'}$ the virtual potential temperature and potential temperature anomalies (deviation from domain mean), respectively, $q_v^{'}$ the water vapor specific humidity anomaly, and ϵ is $\mathrm{M_{air}/M_{h2o}} - 1 =$ 0.61. Overbars indicate domain mean values. Eq. 1 implies that anomalous warming (cooling) and moistening (drying) can both be a source (sink) of buoyancy. Rain evaporation is a source of evaporative cooling and moistening, representing two opposing effects on buoyancy. To investigate which effect is dominant in NE-CSA we analyzed the temperature and moisture anomaly terms in Eq. 1 separately.

3 Results

3.1 Convective Self-Aggregation and Cold Pools

Figure 1 shows the aggregation state of a selection of α cases and their associated cold pools. We show snapshots of precipitable water (PW) at the end of the simulations as an indicator of aggregation, as PW variance has been shown to increase dramatically when convection self-aggregates (Arnold & Randall, 2015; Bretherton et al., 2005). We use the virtual potential temperature anomaly (deviation from domain mean) at the lowest model level as a proxy for cold pools, following Kurowski et al. (2018). Consistent with previous findings, convection self-aggregates when rain evaporation is completely removed for both domain sizes ($\alpha = 0$; Figure 1a, i). Unexpectedly, this behavior is found

to be very singular for near zero α values. The precise threshold depends somewhat on the domain size. For the larger domain the α value for convection to transition from a scattered to an aggregated state is larger: when α was decreased from 0.01 to 0.005 for L128 (Figure 1b, c) and from 0.1 to 0.05 for L256 (Figure 1j, k).

Interestingly, cold pools are largely absent at these α values for both domains (Figure 1f, g for L128; Figure 1n, o for L256), albeit for L256 there might be very weak cold pools for $\alpha = 0.1$. Contrary to what previous studies have found—where convection self-aggregates at all domain sizes in the absence of cold pools—our results suggest that, although they play an important role, cold pools alone cannot explain NE-CSA: convection sometimes does not self-aggregate even in the absence of cold pools. In short, the markedly different aggregation degrees observed are not always accompanied by similarly distinct cold pool strengths. We further observed a quicker CSA development in the smaller domain size. For L128, CSA onset occurred by around day-5 (stabilization around day-20) and for L256 by around day-10 (stabilization around day-30; Figure S1 in Supporting Information).

For the control cases with rain evaporation ($\alpha = 1$) and interactive radiation, convection self-aggregates only in the larger domain (Figure 1l), consistent with previous findings. This is the conventional radiatively-driven aggregation (RDA). RDA took much longer to develop compared to NE-CSA, only developing by around day-35 (Figure S1).

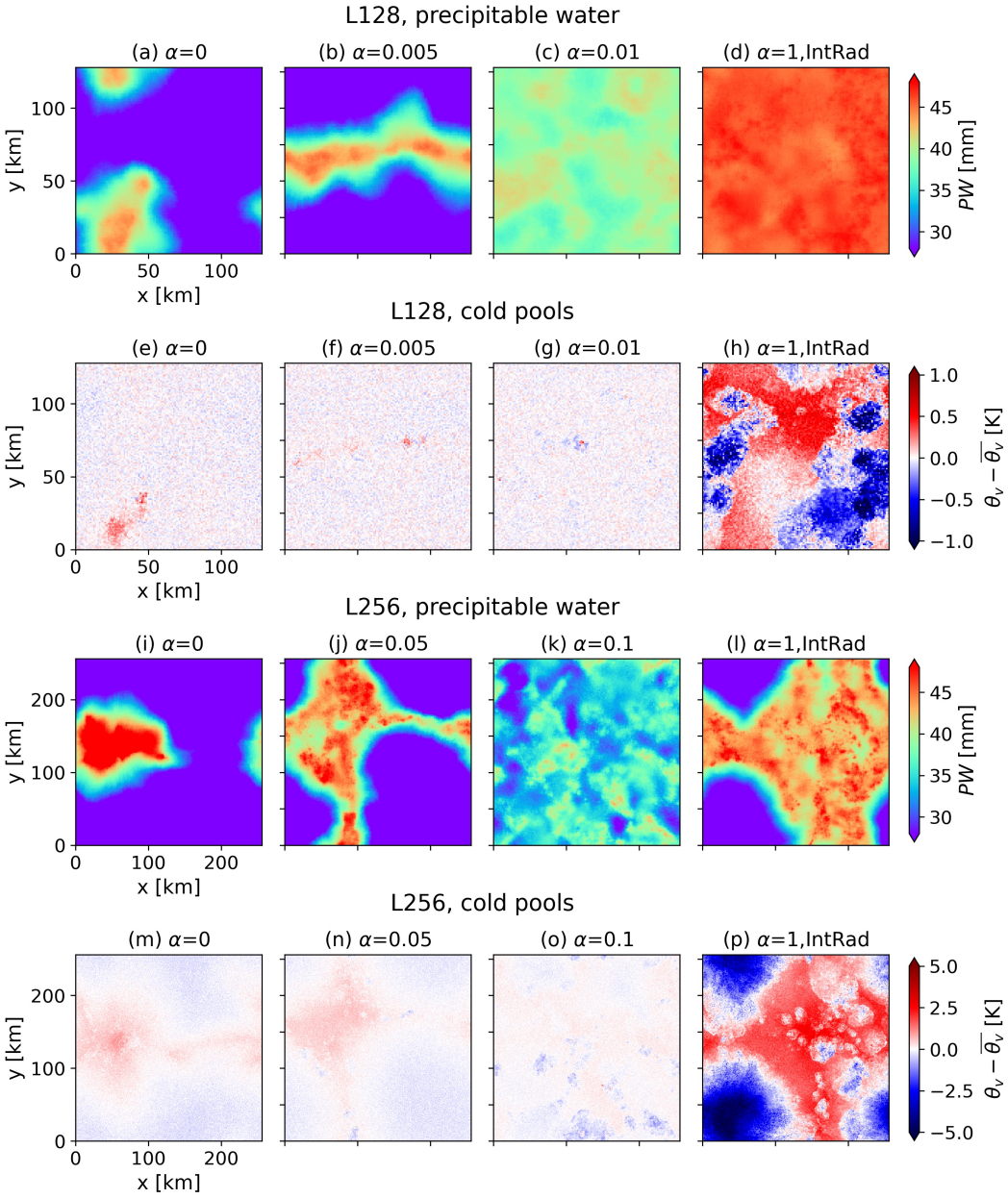

Figure 1. Snapshots at the end of the 40-day simulations of PW and virtual potential temperature anomaly (cold pools) for (a–h) L128 and (i–p) L256.

3.2 Shallow Circulation

It is as yet unclear whether a low-level circulation—a common feature of RDA—would also be present in NE-CSA. A recent study has found that CSA can still develop without a shallow circulation when the subcloud layer is close to saturation (Cerlini et al., 2023), which would prevent precipitation from evaporating, analogous to NE-CSA. To observe the circulation fields we show the MSE and stream function Ψ ranked by column relative humidity (CRH) averaged over the final five days in Figure 2 for selected α cases (see Bretherton et al., 2005, for computation details of Ψ). A low-level circulation is indeed present for the aggregated cases (Figure 2a, b for L128; Figure 2d, e for

L256) but not for the scattered cases (Figure 2c, f). Similar to RDA, this circulation is characterized by a near surface outflow from dry to moist regions, and a partial return flow above the PBL (∼2–3 km). The outflow air has higher MSE compared to the return flow, resulting in an enhanced MSE gradient that over time renders the dry regions drier and moist regions moister. The circulation fields of the aggregated cases also show an intrusion of dry subsidence air from the FT into the PBL (below 1 km) in the driest blocks and an accompanying upward motion in the moistest regions.

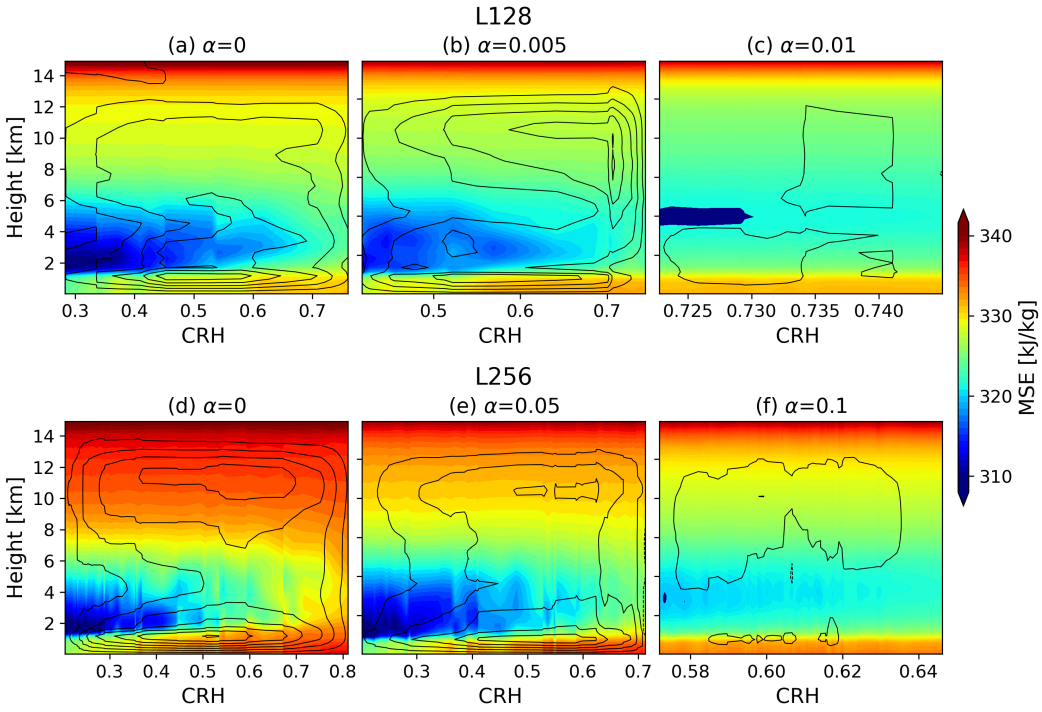

Figure 2. MSE (shading) and stream functions (black contours counterclockwise, intervals of 0.02 kg m^{-2} s^{-1} for L128 and 0.04 kg m^{-2} s^{-1} for L256) averaged over the final five days for the aggregated (a, b, d, e) and scattered (c, f) cases.

3.3 Convectively-Driven Aggregation

Spatial contrasts in radiative cooling in the PBL are believed to be a driving force of the shallow circulation between dry and moist regions (MB15; Naumann et al., 2017). What, then, generates the shallow circulation in NE-CSA where radiation is horizontally homogenized? To investigate this, we compute $\theta_v^{'}$ as a proxy for buoyancy, as a positive buoyancy gradient between the dry and moist areas has been shown to be a prerequisite for the establishment of low-level circulations (Yanase et al., 2022). We show in Figure 3 the time-series of $\theta_v^{'}$ and the contributions of $\theta^{'}$ and $q_v^{'}$ (calculated following Eq. 1), vertically averaged over the lowest 1 km and for the dry and moist patches separately. Note that $\theta_v^{'}$ is very small in the FT, consistent with the WTG assumption (see Figure S2). We define dry and moist regions as grid points where PW is below the 10th and above the 90th percentiles, respectively.

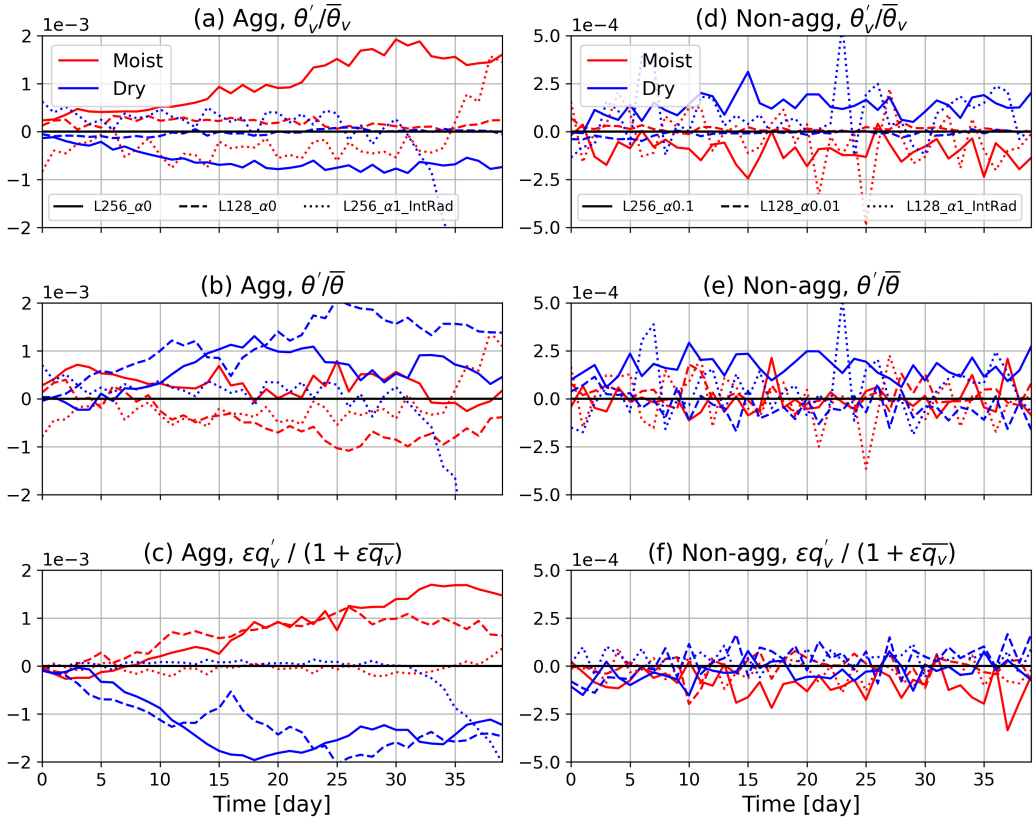

Figure 3. Time evolution of θ_v' (top row) and the contributions of θ' (middle row) and q_v' (bottom row) of the (a–c) aggregated and (d–f) non-aggregated cases. Note the smaller y-axis range for the non-aggregated cases.

We first describe the NE-CSA cases with homogenized radiation. To establish a positive buoyancy gradient, θ_v' of the moist patch must be greater than the dry patch. For the aggregated cases, this is indeed observed for both domain sizes and throughout the simulation period (Figure 3a, solid and dashed curves), indicating that the moist patch is consistently more buoyant than the dry patch, which is conducive to the development of a shallow circulation. In contrast, for the non-aggregated cases (Figure 3d) the moist patch is either negatively (L256) or very weakly positively buoyant (L128), with very small θ_v''s that have a diminishing probability of persistence, evident in the intermittent zero values displayed. This suggests that a large enough positive buoyancy gradient that continuously develops is necessary for aggregation to occur, i.e., both the magnitude of $\Delta\theta_v'$ between the dry and moist patches and its persistence in time matter.

Next we analyze the θ' and q_v' time-series of the aggregated cases. There appears to be three phases in the development of NE-CSA: triggering, intensification, and stabilization. Since radiation and surface fluxes are homogenized, we focus on convective processes, whose effects are more prominent in the moist patch. During the triggering phase (day 0–3 for L128; day 0–7 for L256), the effect of rain evaporation removal is most evident: a reduction in evaporative cooling and moistening results in a net increase in convective heating and drying of the moist patch (positive θ_{dry}' and negative $q_{v,\mathrm{moist}}'$ in Figure 3b, c). Although these are two opposing buoyancy effects, the heating effect prevails, resulting in a positive $\theta_{v,\mathrm{moist}}'$. This indicates that in the triggering phase the additional convective heating of the moist patch plays an important role in kick-starting

NE-CSA. For the scattered cases (Figure 3e, f), there is insufficient reduction in evaporative cooling to set-off CSA.

During the intensification phase (day 3–10 for L128, day 7–17 for L256), the $q_v^{'}$ effects dominate the trend in buoyancy ($\theta_v^{'}$). A gradual increase (decrease) in $q_{v,\mathrm{moist}}^{'}$ ($q_{v,\mathrm{dry}}^{'}$) is observed (Figure 3c). This is indicative of the intrusion of subsidence from the FT into the PBL in the dry patch which causes a growing negative buoyancy, resulting in a divergent flow from the dry patch. This "dry-subsidence feedback" where free-tropospheric dry air invades the PBL has been postulated to be an important mechanism for CSA (Yanase et al., 2022; B. Yang & Tan, 2020). Crucially, the virtual effect of subsidence drying must exceed subsidence warming for the dry patch to remain negatively buoyant. In short, after a sufficiently strong ignition from convective heating in the triggering phase, the virtual effect takes over to intensify CSA. For the scattered case this takeover of virtual effect failed to materialize (Figure 3f) due to weak ignition during the triggering phase.

After the intensification period NE-CSA enters the mature phase. A competing effect between $\theta^{'}$ and $q_v^{'}$ is observed: the virtual effect aids CSA while $\theta^{'}$ contribution opposes it. For both domain sizes the $\theta^{'}$ contribution causes the dry patch to be positively buoyant, and the moist patch to be negatively buoyant for L128 from day 10 onwards and trend towards negative buoyancy for L256 (Figure 3b). The positive $\theta^{'}$ of the dry patch is a result of subsidence warming while the negative $\theta^{'}$ of the moist patch is probably a result of breakthrough evaporative cooling from the FT which gradually intrudes into the PBL due to gravity and inertia (Figure S2, panels b, h). This competing $\theta^{'}$ and $q_v^{'}$ effect explains the need for an almost total removal of rain evaporation in the PBL to, firstly, supply a strong enough boost in the triggering phase, and secondly, to counter the effect of evaporative cooling and ensure $\theta_{v,\mathrm{moist}}^{'}$ remains positive in the mature phase.

The process described above is consistently observed across different α's (Figures S3, S4) and paints a very different picture to the mechanisms underlying RDA (dotted lines in Figure 3). For RDA, the buoyancy gradient remains largely negative during most of the simulation (until ∼day-30), mainly due to negative buoyancy of the moist patch caused by evaporative cooling and positive buoyancy of the dry patch caused by subsidence warming (Figure 3b). Radiative cooling begins to supersede subsidence warming by around day-30 and dramatically decreases the buoyancy of the dry patch through both cooling and subsidence drying. Hence, radiative cooling of the dry patch appears to be the "first-mover" in the initiation of RDA, in contrast to convective heating of the moist patch in NE-CSA. As radiation is a more sluggish process than convection, this also explains the longer time it takes for RDA to develop. Additionally, in contrast to NE-CSA, for RDA $\theta^{'}$ and $q_v^{'}$ work in concert to aid the development of positive buoyancy gradients, once aggregation takes off.

3.4 Domain Size and Radiative Cooling

As investigating the domain size sensitivity of NE-CSA is beyond the scope of this study, we only tested two domain sizes. Nonetheless, the large difference in α threshold for NE-CSA to occur in the two domains is intriguing. We show in Figure 4 the radiative cooling profiles (Q_{rad}; final day average) and time-series of the dry region vertical velocity (averaged over lowest 1 km), as studies have found cloud-radiative feedback to be an important factor contributing to the domain size dependence of CSA (MB15; Muller & Held, 2012). We found Q_{rad} to be generally stronger for L256 than L128. Within each domain size, Q_{rad} is stronger for the aggregated than the scattered cases. This suggests that—even in the absence of spatial inhomogeneity—the magnitude of Q_{rad} still matters for NE-CSA. We postulate that this is due to the stronger subsidence in the dry region induced by a stronger Q_{rad}, which must be balanced by adiabatic warming in the dry region. We confirmed this with sensitivity runs imposing the radiative cooling of the

large domain in the small domain and vice versa: stronger radiative cooling, even homogenized, was found to favor aggregation as expected. The range of CRH increases with domain size (see Figure 2): the driest region is drier in L256 than L128, hence a stronger subsidence is generated. This enables the free-tropospheric dry air to more easily enter the PBL, hence permitting a higher α threshold in L256. This hypothesis also explains why convection self-aggregates in L256 but not L128 for the same α's (0.01, 0.02, 0.05), with similar cold pool strengths in both domains: subsidence is larger for the larger domain ($\overline{w}_{\mathrm{sub,PBL}}$ more negative; Figure 4c).

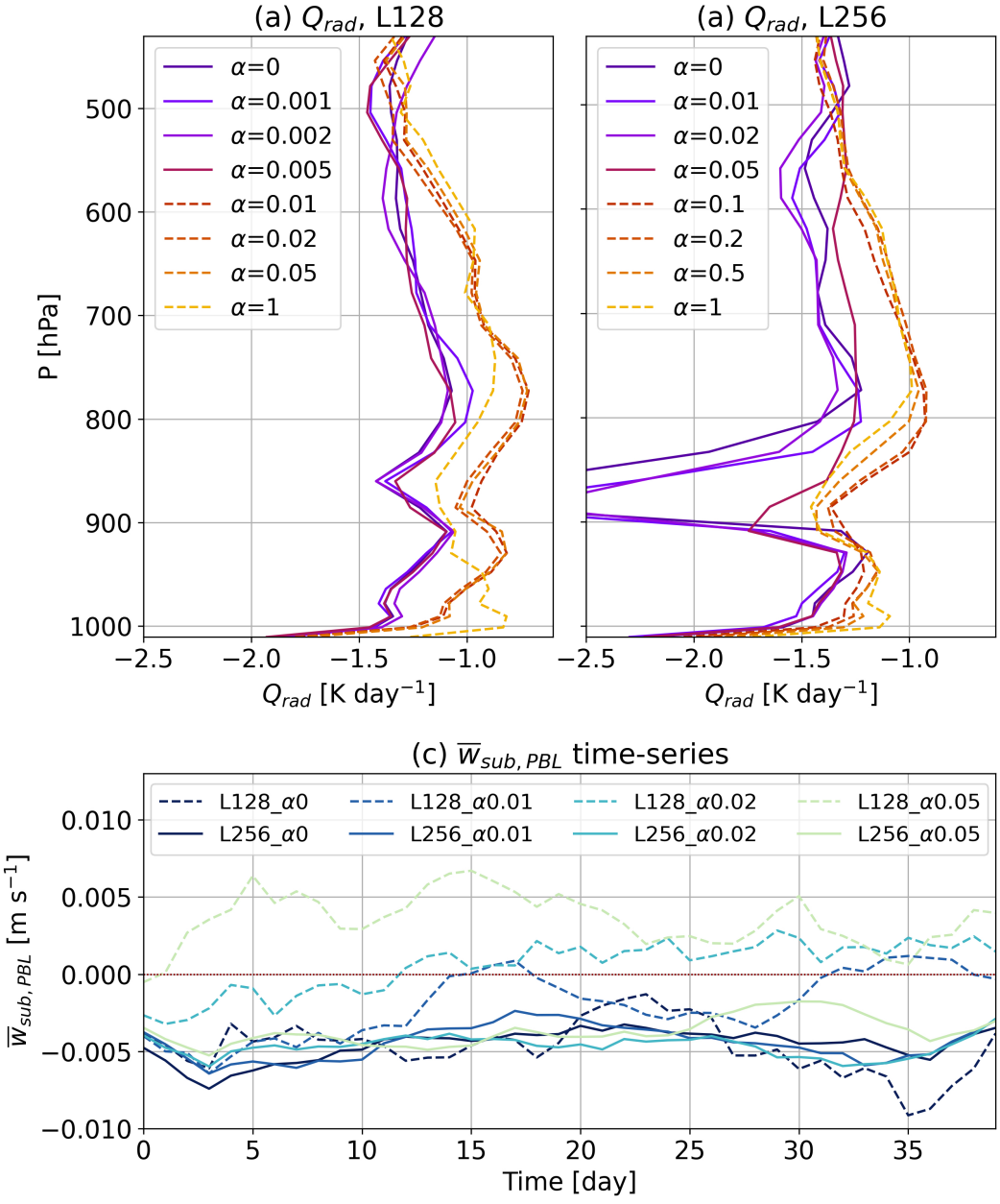

Figure 4. Steady-state Q_{rad} profiles for (a) L128, (b) L256 (up to 400 hPa) and (c) $\overline{w}_{\mathrm{sub,PBL}}$ time-series. Solid and dashed curves in (a, b) indicate aggregated and scattered cases, and in (c) denote L256 and L128, respectively.

Nonetheless, subsidence alone cannot explain the propensity for aggregation. A strong convective heating is still needed to kick-start aggregation. For example, L128_α0 and L128_α0.01 display similar subsidence trajectory in the first 10 days, but aggregation already took off by day-5 for the former while the latter remains non-aggregated (Figure S1), indicating that the ignition from convective heating (determined by α) was insufficient for L128_α0.01. In summary, larger domains generally produce stronger subsidence, and provided sufficient initial boost from convective heating in the moist region, free-tropospheric dry air will enter the PBL in the dry region and CSA will take off.

4 Conclusions

We investigate the physical mechanisms underlying convective self-aggregation (CSA) in the absence of radiative and surface flux feedbacks and with rain evaporation removed or reduced in the PBL, referred to here as no-evaporation CSA (NE-CSA). We progressively reduced rain evaporation by multiplying it by a factor α. We tested two domain sizes: 128 $\times$ 128 km (L128) and 256 $\times$ 256 km (L256).

Our main finding is that NE-CSA only occurs when rain evaporation is entirely (or almost entirely) removed. This is because the temperature and moisture impacts of evaporation reduction oppose each other, making this feedback very sensitive: only when rain evaporation is almost completely removed ($\alpha \approx 0$) can the additional heating trigger aggregation. This type of aggregation is thus likely not relevant to atmospheric organization, except in nearly saturated conditions. Once the initial spark renders the moist patch positively buoyant enough to kick-start CSA, the virtual effect takes over, whereby free-tropospheric dry subsidence descends into the PBL of the dry region and sets CSA in motion until a low-level circulation is able to develop and maintain self-aggregation. In the mature phase the positive contribution of $q_v^{'}$ effects (subsidence drying of dry patch; moisture convergence into moist patch) is counteracted by the negative contribution of $\theta^{'}$ effects (subsidence warming of dry patch; evaporative cooling of moist patch), hence also explaining the need for small α's to attenuate this negative $\theta^{'}$ effect.

In contrast to the dry patch-driven radiatively-driven aggregation (RDA), in NE-CSA the moist and dry regions work in tandem: heating of the moist patch provides the spark to trigger aggregation and subsidence in the dry patch supplies the boost that eventually sets off a shallow circulation that sustains CSA. Given the crucial role of convective heating, we suggest that this type of aggregation should be more appropriately referred to as convectively-driven aggregation (CDA) instead of "moisture-memory aggregation". We also observed that CDA develops significantly quicker than RDA, due to convection being a faster process than radiation.

Further, we found that CDA was able to occur at larger α thresholds in L256 than L128 and cold pools alone cannot explain this domain size dependence, unlike what was suggested in earlier studies. Instead, we postulate that the broadening of the PW range and concomitant increase in radiative cooling is the likelier cause for the relative ease of CDA to occur in the larger domain. The stronger subsidence induced hence allows for a comparatively smaller reduction in evaporative cooling.

Our study expands on the findings of previous studies and lends nuance to established theories about CSA, which have predominantly focused on the mechanisms underlying dry patch expansion. By illuminating the role of convective heating, we think that the physical processes in the moist patch are also worthy of note and should be taken into account when considering the numerous environmental conditions under which aggregation can occur. Our idealized study represents an important step towards understanding the effects of rain evaporation in influencing convective organization.

5 Open Research

The data, scripts and model source codes and files required to reproduce the results described in this manuscript are available at `https://zenodo.org/record/8369510` [DOI: `https://doi.org/10.5281/zenodo.8369510`]

Acknowledgments

YLH is supported by funding from the European Union's Horizon 2020 research and innovation programme under the Marie Skłodowska-Curie Grant Agreement No. 101034413. CM gratefully acknowledges funding from the European Research Council (ERC) under the European Union's Horizon 2020 research and innovation program (Project CLUSTER, Grant Agreement No. 805041). The authors warmly thank Steven Sherwood, Jiawei Bao, Bidyut Goswami, and Martin Janssens for stimulating and helpful discussions.

References

Arnold, N. P., & Randall, D. A. (2015). Global-scale convective aggregation: Implications for the madden-julian oscillation. *Journal of Advances in Modeling Earth Systems*, *7*(4), 1499–1518.

Bretherton, C. S., Blossey, P. N., & Khairoutdinov, M. (2005). An energy-balance analysis of deep convective self-aggregation above uniform sst. *Journal of the atmospheric sciences*, *62*(12), 4273–4292.

Carstens, J. D., & Wing, A. A. (2020). Tropical cyclogenesis from self-aggregated convection in numerical simulations of rotating radiative-convective equilibrium. *Journal of Advances in Modeling Earth Systems*, *12*(5), e2019MS002020.

Cerlini, P. B., Saraceni, M., & Silvestri, L. (2023). Competing effect of radiative and moisture feedback in convective aggregation states in two crms. *Journal of Advances in Modeling Earth Systems*, *15*(2), e2022MS003323.

Craig, G. C., & Mack, J. M. (2013). A coarsening model for self-organization of tropical convection. *Journal of Geophysical Research: Atmospheres*, *118*(16), 8761–8769.

Cronin, T. W., & Wing, A. A. (2017). Clouds, circulation, and climate sensitivity in a radiative-convective equilibrium channel model. *Journal of Advances in Modeling Earth Systems*, *9*(8), 2883–2905.

Holloway, C. E., & Woolnough, S. J. (2016). The sensitivity of convective aggregation to diabatic processes in idealized radiative-convective equilibrium simulations. *Journal of Advances in Modeling Earth Systems*, *8*(1), 166–195.

Jeevanjee, N., & Romps, D. M. (2013). Convective self-aggregation, cold pools, and domain size. *Geophysical Research Letters*, *40*(5), 994–998.

Khairoutdinov, M. F., & Emanuel, K. (2018). Intraseasonal variability in a cloud-permitting near-global equatorial aquaplanet model. *Journal of the Atmospheric Sciences*, *75*(12), 4337–4355.

Khairoutdinov, M. F., & Randall, D. A. (2003). Cloud resolving modeling of the arm summer 1997 iop: Model formulation, results, uncertainties, and sensitivities. *Journal of the Atmospheric Sciences*, *60*(4), 607–625.

Kurowski, M. J., Suselj, K., Grabowski, W. W., & Teixeira, J. (2018). Shallow-to-deep transition of continental moist convection: Cold pools, surface fluxes, and mesoscale organization. *Journal of the Atmospheric Sciences*, *75*(12), 4071–4090.

Mapes, B., & Neale, R. (2011). Parameterizing convective organization to escape the entrainment dilemma. *Journal of Advances in Modeling Earth Systems*, *3*(2).

Muller, C., & Held, I. M. (2012). Detailed investigation of the self-aggregation of convection in cloud-resolving simulations. *Journal of the Atmospheric Sciences*, *69*(8), 2551–2565.

Muller, C., & Romps, D. M. (2018). Acceleration of tropical cyclogenesis by self-aggregation feedbacks. *Proceedings of the National Academy of Sciences*, *115*(12), 2930–2935.

Muller, C., Yang, D., Craig, G., Cronin, T., Fildier, B., Haerter, J. O., ... others (2022). Spontaneous aggregation of convective storms. *Annual Review of Fluid Mechanics*, *54*, 133–157.

Naumann, A. K., Stevens, B., Hohenegger, C., & Mellado, J. P. (2017). A conceptual model of a shallow circulation induced by prescribed low-level radiative cooling. *Journal of the Atmospheric Sciences*, *74*(10), 3129–3144.

Nissen, S. B., & Haerter, J. O. (2021). Circling in on convective self-aggregation. *Journal of Geophysical Research: Atmospheres*, *126*(20), e2021JD035331.

Patrizio, C. R., & Randall, D. A. (2019). Sensitivity of convective self-aggregation to domain size. *Journal of Advances in Modeling Earth Systems*, *11*(7), 1995–2019.

Shamekh, S., Muller, C., Duvel, J.-P., & d'Andrea, F. (2020). Self-aggregation of convective clouds with interactive sea surface temperature. *Journal of Advances in Modeling Earth Systems*, *12*(11), e2020MS002164.

Sobel, A. H., Nilsson, J., & Polvani, L. M. (2001). The weak temperature gradient approximation and balanced tropical moisture waves. *Journal of the atmospheric sciences*, *58*(23), 3650–3665.

Tompkins, A. M. (2001). Organization of tropical convection in low vertical wind shears: The role of water vapor. *Journal of the atmospheric sciences*, *58*(6), 529–545.

Tompkins, A. M., & Craig, G. C. (1998). Radiative–convective equilibrium in a three-dimensional cloud-ensemble model. *Quarterly Journal of the Royal Meteorological Society*, *124*(550), 2073–2097.

Tompkins, A. M., & Semie, A. G. (2017). Organization of tropical convection in low vertical wind shears: Role of updraft entrainment. *Journal of Advances in Modeling Earth Systems*, *9*(2), 1046–1068.

Windmiller, J. M., & Craig, G. C. (2019). Universality in the spatial evolution of self-aggregation of tropical convection. *Journal of the Atmospheric Sciences*, *76*(6), 1677–1696.

Wing, A. A. (2019). Self-aggregation of deep convection and its implications for climate. *Current climate change reports*, *5*, 1–11.

Wing, A. A., & Cronin, T. W. (2016). Self-aggregation of convection in long channel geometry. *Quarterly Journal of the Royal Meteorological Society*, *142*(694), 1–15.

Wing, A. A., Emanuel, K., Holloway, C. E., & Muller, C. (2018). Convective self-aggregation in numerical simulations: A review. *Shallow clouds, water vapor, circulation, and climate sensitivity*, 1–25.

Wing, A. A., & Emanuel, K. A. (2014). Physical mechanisms controlling self-aggregation of convection in idealized numerical modeling simulations. *Journal of Advances in Modeling Earth Systems*, *6*(1), 59–74.

Wing, A. A., Stauffer, C. L., Becker, T., Reed, K. A., Ahn, M.-S., Arnold, N. P., ... others (2020). Clouds and convective self-aggregation in a multimodel ensemble of radiative-convective equilibrium simulations. *Journal of Advances in Modeling Earth Systems*, *12*(9), e2020MS002138.

Yanase, T., Nishizawa, S., Miura, H., Takemi, T., & Tomita, H. (2020). New critical length for the onset of self-aggregation of moist convection. *Geophysical Research Letters*, *47*(16), e2020GL088763.

Yanase, T., Nishizawa, S., Miura, H., Takemi, T., & Tomita, H. (2022). Low-level circulation and its coupling with free-tropospheric variability as a mechanism of spontaneous aggregation of moist convection. *Journal of the Atmospheric Sciences*, *79*(12), 3429–3451.

Yang, B., & Tan, Z.-M. (2020). The initiation of dry patches in cloud-resolving con-

vective self-aggregation simulations: Boundary layer dry-subsidence feedback. *Journal of the Atmospheric Sciences*, *77*(12), 4129–4141.

Yang, D. (2018). Boundary layer diabatic processes, the virtual effect, and convective self-aggregation. *Journal of Advances in Modeling Earth Systems*, *10*(9), 2163–2176.

Yang, D. (2019). Convective heating leads to self-aggregation by generating available potential energy. *Geophysical Research Letters*, *46*(17-18), 10687–10696.